Heliyon 9 (2023) e19230

Contents lists available at ScienceDirect

Heliyon

journal homepage: www.cell.com/heliyon

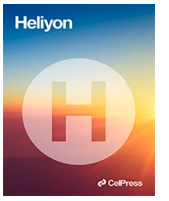

Polyacrylic acid/ polyvinylpyrrolidone hydrogel wound dressing containing zinc oxide nanoparticles promote wound healing in a rat model of excision injury

Mohsen Shahrousvand [a], Seyyedeh Sahra Mirmasoudi [b,*], Zahra Pourmohammadi-Bejarpasi [b], Alireza Feizkhah [b], Mohammadreza Mobayen [b], Mojtaba Hedayati [b], Mahsa Sadeghi [b], Mojdeh Esmaelzadeh [b], Fatemeh Beygom Mirkatoul [b], Solma Jamshidi [b]

[a] Caspian Faculty of Engineering, College of Engineering, University of Tehran, Rezvanshahr, P.O. Box: 43841-119, Guilan, Iran
[b] Burn and Regenerative Medicine Research Center, Guilan University of Medical Sciences, Rasht, Iran

ARTICLE INFO

Keywords:
Wound dressing
Hydrogel
ZnONPs
Polyvinylpyrrolidone (PVP)
Polyacrylic acid (PAA)
Excisional wound

ABSTRACT

Developing and designing efficient wound dressings have gained increasing attention and shown beneficial results in improved wound healing effects. This study was conducted to improve wound healing properties and introduce a novel potential wound dressing. A novel hydrogel based on polyvinylpyrrolidone/poly acrylic acid containing Zinc oxide nanoparticles was prepared as an antibacterial wound dressing and examined in a rat excisional wound model. This hydrogel prepared by free radical polymerization using potassium persulfate (KPS) as an initiator, N, N-methylene bisacrylamide (MBA) as a cross-linker, poly acrylic acid (PAA) as a monomer in the presence of polyvinylpyrrolidone (PVP) and Zinc oxide nanoparticles (ZnO NPs). Analyses such as Scanning Electron Microscope (SEM), Fourier-transform infrared spectroscopy (FTIR), X-ray diffraction analysis (XRD), and Thermal gravimetric analysis (TGA) were used to study morphology structure. After choosing the optimal sample, in vivo characterization of excisional wound injury on a rat model was done. The healing rate and histological analysis were calculated and compared among the groups. The therapeutic potential of the PAA-PVP-ZnO-%2 was investigated in a rat model of excisional injury compared to the control group. Results showed that the polyacrylic acid/polyvinylpyrrolidone hydrogel wound dressing containing zinc oxide nanoparticles accelerated wound contraction, had antibacterial effects, and promoted wound healing compared to other groups.

1. Introduction

Skin disorders such as burns, excisional injuries, bedsores, diabetic wounds, and trauma are among the most important causes of disability and death of patients [1]. Long-term disability, deformity, mortality, and socioeconomic costs are imposed on patients, families, and communities in both developed and developing countries due to these injuries [2]. Related complications include ulceration, infection, organ failure, ischemia [3], impaired metabolic, inflammatory, endocrine factors, and immune responses that may

* Corresponding author.
E-mail address: Mirmasoudisahra.sm@gmail.com (S.S. Mirmasoudi).

https://doi.org/10.1016/j.heliyon.2023.e19230
Received 8 April 2023; Received in revised form 29 July 2023; Accepted 16 August 2023
Available online 17 August 2023

predispose patients to malnutrition and weakness. In the wound healing process, muscle wasting, severe weight loss, and recurrent infections lead to long-term hospitalization, and treatment of these complications requires the presence of specialized wound care units [3]. It is worth mentioning that one of the serious problems of wounds is secretions related to infection. Therefore, choosing a dressing with various features like absorption of excess fluids, maintaining a moist environment, biocompatibility, antimicrobial protection, minimal frequency of dressing change, maintenance of appropriate temperature, reduced patient pain, etc., are essential [4–6]. According to the aforementioned, hydrogels have high maneuverability in design compared to other wound dressings, and they are hydrophilic polymers based on a three-dimensional network capable of absorbing large amounts of water or biofluids and are composed of two components, water-soluble polymers, and cross-linkers, that make the hydrogel insoluble in water. They can swell in water and retain a certain amount of water when immersed in an aqueous solution. The polymer scaffold can absorb a minimum of 20% and a maximum of 99% by water weight [7–9]. Hydrogels unlike other synthetic materials are similar to living tissues in soft and rubbery surface, structure, and physicochemical properties [10]. Hydrogels are utilized in different medical applications like contact lenses, tissue engineering, and wound dressings, as well as the release of therapeutic agents due to their extracellular matrix (ECM) structure and capability at absorbing water [11]. Hydrogels can be selected from many factors, such as the primary source of the hydrogel (synthetic or natural polymer), the structure of the hydrogel (copolymer network, homopolymer network, and permeation network), cross-linking method (chemical and physical), hydrogel load (Cationic and Anionic) and biocompatibility (biodegradable, biostable) [12–17]. Poly (acrylic acid) (PAA) and Poly-(N-vinyl-2-pyrrolidone) (PVP) are water-soluble polymers with excellent biocompatibility. They have a high ability to absorb and retain water. However, they are the basis of a class of materials called superabsorbents.

PVP may take up as much water as 100 times its own weight. This aids in maintaining the wound's moisture, which is crucial for healing. A moist wound will heal more quickly than a dry one and is less prone to contract an infection. Because PVP is a semi-permeable barrier, it allows oxygen and nutrients to pass through while blocking the entry of germs and other pollutants. The mending process requires nutrition and oxygen. Nutrients are required for tissue repair and cell growth and division, which depend on oxygen. PVP can aid in the debridement of wounds by absorbing exudate and dead tissue [18]. This helps to clean up the wound's surroundings and remove germs and other pollutants. Exudate and dead tissue can be a haven for bacteria and impede healing. PVP can aid in defending wounds against additional damage or infection. The wound may be kept clean and moist, which is important for healing. PVP can be a physical barrier to stop further harm to the wound. By absorbing exudate, it can also assist in keeping the wound clean and moist [19].

It is crucial to understand that PVP does not heal wounds. It is a type of wound dressing that can aid in promoting recovery and reducing infection risk.

When it comes to wound healing, PAA can encourage Antibacterial activity, Moisture equilibrium, Inhibition of proteases, Collagen deposition, Re-epithelialization, Formation of granulation tissue, and Vascularization. PAA can destroy the cell membranes of bacteria by rupturing them. This can hasten the healing process and help avoid infection [20]. It is hydrophilic, attracting water. This can assist in maintaining wound moisture, which is crucial for healing. Proteases are enzymes that can degrade proteins like collagen, and PAA can stop them from doing so. This can aid in preventing further injury to the wound and speed up recovery. The protein collagen, which is necessary for wound healing, can be stimulated by PAA. PAA can encourage the development of fresh skin cells essential for healing wounds. PAA can encourage the growth of granulation tissue, which aids in healing wounds and lays the groundwork for developing new skin. It can encourage the development of new blood vessels essential for supplying the wound with oxygen and nutrients [21,22].

Therefore, these dressings are easily removed from the wound due to the wet surface and low adhesion to the wound, which is an important factor in the clinical management of injury [23]. On the other hand, due to the importance of infectious control of wounds, Studies have shown that various factors introduce into the wound structure to improve the antibacterial properties of the wound. Zinc oxide nanoparticles are of this category [24]. Unique properties of ZnO nanoparticles, such as chemical and photochemical stability, high catalytic effects, resistance to ambient temperature, low toxicity, and their inclusion in the category of GRAS (Generally recognized as safe) materials, cause widespread use compared to other new nanoparticles [25].

Numerous advantages of zinc oxide nanoparticles (ZnO NPs) on wound healing have been demonstrated in articles, including antibacterial, anti-inflammatory, pro-regenerative, biocompatible antimicrobial, non-toxic, and antioxidant actions. Because of these qualities, they are a prospective contender for creating novel wound healing therapies [26].

By producing reactive oxygen species (ROS), ZnO NPs can eliminate bacteria. ROS can harm bacterial cell membranes, which results in cell death. ZnO NPs can increase the synthesis of cytokines that cause inflammation, including interleukin-1beta (IL-1beta) and tumor necrosis factor-alpha (TNF-alpha). These cytokines play a role in recruiting immune cells to the wound site and other early phases of wound healing. ZnO NPs can promote fibroblast proliferation, a process by which cells that make collagen and other proteins required for wound healing proliferate. ZnO NPs can also boost the expression of genes related to wound healing, like the collagen gene. ZnO NPs have antioxidant action because they can scavenge free radicals and unstable chemicals that harm tissues and cellular structures. Bacteria, inflammation, and other causes can all result in the production of free radicals. ZnO NPs can aid in healing by preventing cell damage from free radicals [27,28]. Of note, an antibacterial wound dressing is utilized to cover the wound bed; it acts as a physical barrier for prevention of pathogens from entering the wound or killing invading microorganisms. Furthermore, by stimulating the immune system and fibroblast/keratinocyte migration, these types of wound dressing aid in excisional wound and bacteria-infected diabetic wound healing [29–32].

The objective of this study was to create an innovative hydrogel composed of polyvinylpyrrolidone/polyacrylic acid containing ZnO nanoparticles, which possesses multiple properties to facilitate an optimal environment for wound healing. We examined the topography, swelling and deswelling ratios, thermal stability, X-ray diffraction patterns, antibacterial properties, and cytotoxicity effects of the hydrogel. Additionally, the performance of the PAA-PVP-ZnO hydrogel was assessed using excisional wound models in

rats, and clinical and histological observations were gathered. The results showed that the nontoxic hydrogel with antibacterial properties promoted wound healing. Hence, we hope PAA-PVP-ZnO-%2 hydrogels have a promising strategy for wound healing, drug delivery, and other biomedical applications in future.

2. Materials and methods

2.1. Materials

Before use, the monomer, acrylic acid (AA, Merck, 99%), was distilled at vacuum, and the cross-linker *N*, *N*′-methylene-bis-acrylamide (MBA, Merck, 99%), was used as received. A radical polymerization redox system contained potassium persulphate (KPS, 99%) was procured from Merck, and ZnO nanoparticles powder with an average particle diameter of about 20 nm were obtained from Aldrich. Distilled water was utilized in all stages.

2.2. Synthesis of PAA-PVP semi-IPNs with various PVP content

The hydrogels preparation was based on the values listed in Table 1. First, PVP was dissolved in distilled water, and then other compounds were added to it. Finally, the ingredients were poured into pre-heated silicone molds (Inside the oven at 70 °C), and the lid of the mold was covered.

2.3. Synthesis of PAA-PVP semi-IPNs with various ZnO content

Based on the samples synthesized in the previous step, the best sample was selected, and different percentages (0%, 1%, 2%, and 4%) of nanoparticles were added.

2.4. Characterization

2.4.1. Swelling and deswelling ratio

Samples were dried at 70 °C and evaluated for the swelling rate described in the results. The dried hydrogel weight was first measured before being immersed in 30 ml distilled water and kept at standard room temperature (25 °C) until the swelling balance was reached. The specimens were taken out of the water at specific times (200, 400, 600, 800, 1000, 1200, 1400, 1600, and 1800 min), and the excess water was removed with filter paper and measured again. To calculate the swelling degree, we have:

$$\text{Degree of Swelling (\%)} = (\text{Weight of swollen–Weight of polymer})/\text{Weight of polymer} \times 100$$

2.4.2. Fourier transform infrared spectroscopy analysis

FTIR spectra determined the chemical structure of the dried PAA-PVP hydrogel were recorded in the range 600–4000 cm^{-1} on an Equinox 55 FTIR spectrometer with 100 scans to show the interaction between PAA polymers with different percentages of PVP.

2.4.3. Scanning electron microscopy analysis

Using Scanning Electron Microscopy (SEM), we analyzed the surface fracture of the hydrogel containing PAA with different percentages of PVP via an AIS 2100 scanning electron microscope (Seron Technology, Korea) with a 26 kV magnification.

2.4.4. Thermogravimetric analysis of hydrogels without nanoparticles

Thermogravimetric (TGA) is one of the common methods for determining the thermal stability of various materials and the degradation of polymers at various temperatures. Because hydrogel thermal stability is critical for practical applications, TGA data were collected using a PerkinElmer STA 6000 thermal analyzer. Heating the samples at 10 °C/min from room temperature to 600 °C, the prepared hydrogel's thermal stability was experimentally investigated.

2.4.5. X-ray diffraction analysis

The X-ray diffraction (XRD) patterns of (PAA-PVP-7.5-ZnO, PAA-PVP-7.5, and ZnO nanoparticles) hydrogels were assessed in a

Table 1
Recipe of PAA/PVP semi-IPN hydrogel synthesis.

Name of Sample	Water (g)	PVP	AA (g)	MBA (g)	KPS (g)
PAA-PVP-0	10	0	3	0.01	0.04
PAA-PVP-2.5	10	0.25	3	0.01	0.04
PAA-PVP-5	10	0.5	3	0.01	0.04
PAA-PVP-7.5	10	0.75	3	0.01	0.04
PAA-PVP-10	10	1	3	0.01	0.04

diffractometer with the D8-Advance of the Bruker company in Germany.

2.4.6. Antibacterial test

PAA-PVP-7.5-ZnO-2% and PAA-PVP-7.5 were tested on *Staphylococcus aureus* (gram-positive) and Pseudomonas arauginosa (gram-negative) by the zone of inhibition experiment. Pouring Muller-Hinton agar onto the petri dishes, it was let for solidification. Bacteria were spread on two different plates uniformly. Hydrogels were placed gently over the agar gel. To check the zone of inhibition, the plates were incubated for 24 h at 37 °C. Gentamycin disc (10 μg dose) is used as a positive control in each plate.

2.4.7. Cytotoxicity MTT assay

The cytotoxicity of PAA-PVP hydrogel wound dressing containing zinc oxide nanoparticles on human dermal fibroblast cell line (HDF) was evaluated by MTT assay Kit. The HDF cells were cultured in DMEM high glucose growth medium with 10% FBS in an incubator with 5% CO2 at 37 °C. For this purpose, 5×10^4 cells were cultured in 96 well plates and treated by PAA-PVP-7.5-ZnO-2% extracts for 24 and 48 h. The culture medium in the wells was then removed and rinsed with PBS. Adding the MTT solution to the wells, incubation was performed for 3h. After removing the MTT solution and washing the wells, 100 μl of DMSO was added to each well. Ultimately, an ELISA reader was used to measure the optical density (OD) of content in the range of 540 nm [33].

2.4.8. Animal studies

In the current work, 30 male Wistar rats (280–300 g) were utilized. All animal procedures were based on the National Committee for Ethics in Biomedical Research's Animal Care Committee guidelines (IR.GUMS.REC.1400.425). The animals were holded individually in a standard environment temperature (23 °C), and a regular 12:12 light/dark cycle.

2.4.9. Excisional wound model in rat

Excisional wound was developed according to Pourmohammadi-Bejarpasi et al. study [34]. Briefly, anesthesia was administrated by intraperitoneal injection (Ketamine (70 mg/kg) and Xylazine (7 mg/kg)). First, the dorsal area of the rats was shaved and disinfected. Next, the sterile surgical punch was used to create a 1.5 cm diameter excisional wound. Then, PAA-PVP-7.5-ZnO-2% hydrogel was applied to the wound area, and covered with a transparent wound dressing (Comfeel Plus, Coloplast, Denmark). The rats were divided into two groups, including (1) Control (Ctrl; those with excisional wound without any treatment) and (2) intervention (PAA-PVP-7.5-ZnO-2%; the rats with excisional wound that received PAA-PVP-7.5-ZnO- 2% hydrogel).

2.4.10. Wound healing rate

At 0, 7, and 21 days post-surgery, the wound contraction rate was photographed using a digital camera (Canon EOS 2000D, Japan). Standardization of wound size was done with a ruler. Wound area size was measured using Image J software (NIH V.1.8.0_112 USA), and the wound contraction rate was calculated according to the following equation:

$$\text{Wound Contraction } (\%) = ((\text{Initial wound size - specific wound size})/\text{Initial wound size}) \times 100$$

2.4.11. Histological investigations

An overdose of Ketamine/Xylazine was used to sacrifice the rats. Biopsies from wound area along with nearby normal skin were fixed in 10% formaldehyde for at least 72 h, then, dehydration process was done. Finally, the paraffin-embedded samples were obtained in 5 μm sections using a microtome. Following that, the slides were stained with hematoxylin and eosin and Masson's trichrome dyes in accordance with standard laboratory protocols.

2.4.12. Statistical analysis

GraphPad Prism software V.8.0.2 (NIH, USA) was used for data analysis. The Tukey's post hoc *t*-test, and two-way ANOVA were used for multiple comparisons. The Shapiro-Wilk test was used to evaluate the normalization of the data. Furthermore, Kruskal-Wallis statistical and One way ANOVA tests were utilized for analyzing the findings, considering the P values of less than 0.05 as significant.

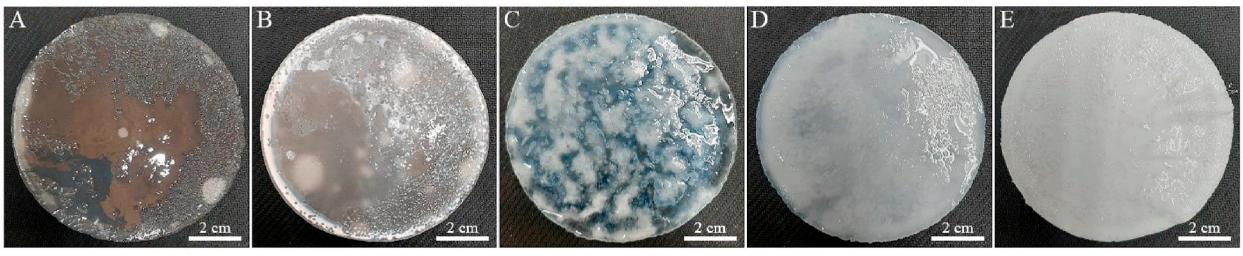

Fig. 1. A visual comparison of PAA-PVP hydrogels with different concentrations of PVP. A) PAA-PVP-0, B) PAA-PVP-2.5, C) PAA-PVP-5, D) PAA-PVP-7.5, E) PAA-PVP-10.

3. Results

3.1. Visual appearance and composition of PAA-PVP hydrogels with different concentrations of PVP

A visual comparison of PAA-PVP hydrogels is shown in Fig. 1(A–E). PAA-PVP hydrogels were synthesized with different percentages of PVP, respectively (0, 2.5, 5, 7.5, and 10). Hydrogel samples were synthesized based on data reported in Table 1. As shown in Fig. 1, by increasing the amount of polyvinylpyrrolidone from 0 to 10%, the transparency of the samples decreases, and they gradually become translucent to opaque so that the sample containing 10% PVP is completely opaque. The samples had good stability and were further investigated to evaluate the degree of swelling and deswelling.

3.2. Swelling and deswelling ratio results

The swelling rate of hydrogels as a wound dressing is a critical parameter that keeps the surface of wound moist. Of course, this amount of moisture absorption should not be excessive, leading to a decrease in moisture on the wound's surface [35]. Therefore, the amount of absorption and transmittance should be optimal. The swelling and deswelling rate of PAA-PVP hydrogel at different time intervals is represented in Fig. 2 (A&B). Two graphs, a and b, show the swelling and deswelling of hydrogel synthesized with different percentages of PVP, respectively. Water absorption results in a neutral environment (pH = 7) indicate that the sample with more PVP has the lowest amount of swelling; its swelling increases with the decrease of PVP in the hydrogel the lowest amount of swelling; their swelling increase with the decrease of PVP in hydrogel structure. This feature can be related to the hydrogel interactions between the vinylidene groups in the PVP structure and the hydroxyl groups in the polyacrylic acid structure. Therefore, PAA-PVP semi--interpenetrating networks have physical hydrogen interactions in addition to the chemical cross-link caused by methylene bisacrylamide, so these hydrogels can be considered IPN. The results of some studies show that the swelling and deswelling pattern varies depending on the percentage of PVP and PAA [36]. This interaction has also caused slower transmission. So that in diagram b, the sample with the highest amount of PVP hardly released the water that was absorbed because of the same strong hydrogen interactions as well as the chemical cross-link in acrylic acid. So, drying and permeability humidification is done slowly. Therefore, it seems that the 7.5% PVP sample had shown good water absorption and permeability, so the 7.5% PVP sample was chosen as the optimal sample for the following tests.

3.3. FTIR analysis results

The FTIR spectra of PAA polymers with different percentages of PVP are shown in Fig. 3. The spectrum of the FTIR test confirmed interactions in the structure of PAA-PVP, as shown in the article by Wu and his colleagues [37]. For the PAA-PVP-0 sample, (CH2) bands were observed at 2920-3450 cm^{-1} and 1390-1280 cm^{-1}; it should be noted that absorption at 1630 cm^{-1} was a mixed mode with participation of both (C═O) and (C–N) in PVP, where the absorption of C═O in PVP was much stronger. The presence of PAA dimer formation with a characteristic C═O absorption at 1630 cm^{-1} and a broad OH absorption band at 3000 cm^{-1} was evident, indicating that both dimer and monomer OH groups were present in PAA-PVP-0 under pH conditions. Also, studies on the FTIR spectrum of PAA-PVP hydrogels have been reported, which are almost similar to the analyzes of the synthesized samples [36]. Appropriately, these monomeric OH groups facilitate hydrogen bonding interactions with other functional groups (such as C═O). Only a weak peak at 1722 cm^{-1} was observed for the PVP-containing samples. The absence of this band in the PAA-PVP-0 hydrogel showed that the hydrogen bond dimers between the carboxyl groups of PAA were disrupted, while the broadening of the 1653 cm^{-1} band was attributed to the hydrogen bonds formed between COOH and C═O in PAA.

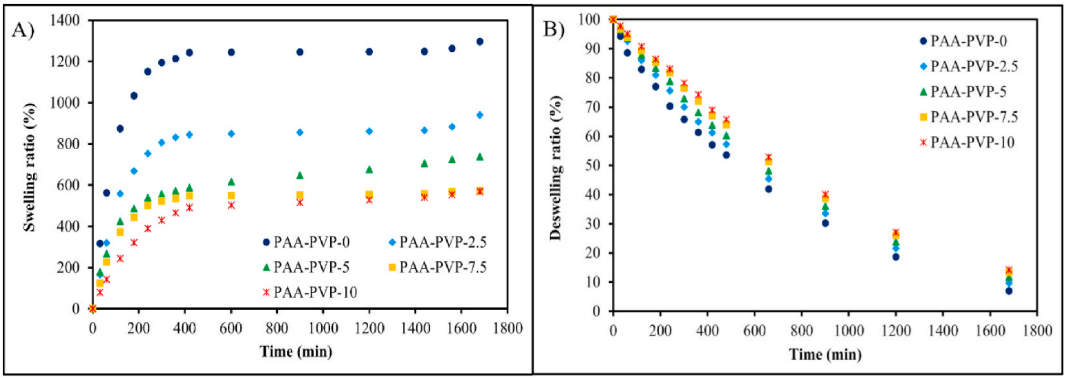

Fig. 2. Swelling and deswelling behavior of hydrogel synthesized with different concentration of PVP in water (pH 7) at room temperature. A) Swelling ratio, B) Deswelling ratio.

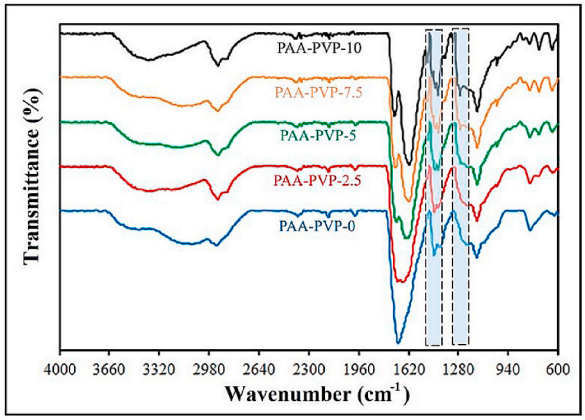

Fig. 3. The FTIR spectra of PAA polymers with different percentages of PVP.

3.4. SEM analysis results

The ultrastructure of PAA-PVP with different concentrations of PVP is shown in Fig. 4 (A–E) The electron microscope test did not show phase separation. As shown in the SEM images, their fracture surface showed a smooth fracture surface and did not show any phase separation of the acrylic acid and PVP polymers, which confirmed the excellent interaction between the two PVP-PAA polymers. It is worth mentioning that PVP has a cationic structure, and PAA has an anionic structure; strong polar interactions are established between them [37,38].

3.5. TGA analysis results

The thermal stability of PAA-PVP with different concentrations of PVP was investigated by TGA Fig. 5A. The TGA analysis of the samples shows thermal stability, although their operating temperature is 37 °C. The reason for evaluating this test is to evaluate the interaction of chains, structures, and their characteristics. As illustrated in Fig. 5A The sample with the lowest PVP (PAA-PVV-0) has a declining drop in the range of 100° due to the evaporation of water in its structure. The next decline is observed after 200 °C due to the destruction of side groups of acrylic acid. At temperatures above 400, it also leads to the destruction of the main chain of the backbone polymer [39,40]. Adding PVP delay the degradation of the main chain in a two-step. Steps are related to acrylic acid and PVP. So, TGA analysis confirmed the perfect PAA-PVP interaction from this test. It should be noted that increasing the amount of PVP reduces the declining drop at 100°. This action is similar to the swelling test, in which the increase in PVP causes a decrease in swelling. As illustrated in Fig. 5B, Comparison of TGA analysis between PAA-PVP-7.5 and PAA-PVP-7.5-ZnO-2% represents that the presence of ZnO in the hydrogel has created chemical resistance in the hydrogel structure, which is due to the positive interaction of ZnO with carboxyl groups (C═O) present in acrylic acid that create an ionic bond between the chains of polyacrylic acid and make the hydrogel more networked. In other words, the comparison indicates that after a temperature of 450°, the PAA-PVP-7.5-ZnO-2% diagram is higher than the PAA-PVP-7.5. Because zinc oxide, as a mineral component, remains in the structure of hydrogels. When the hydrogel is degraded, carbon and carbohydrate materials are released as a gas, and mineral materials remain in the structure.

3.6. XRD analysis results

X-Ray diffraction (XRD) as a crystallographic structure, chemical composition, and physical properties analysis is demonstrated in

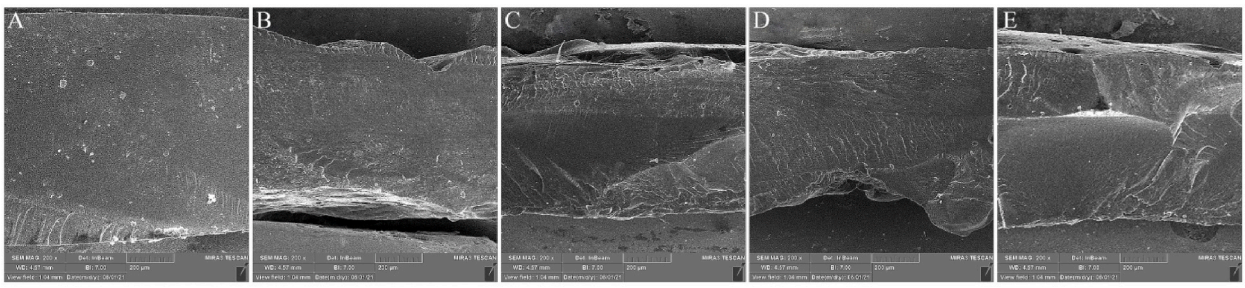

Fig. 4. SEM images illustrating the structure of the surfaces of hydrogels with different percentages of PVP. A) PAA-PVP-0, B) PAA-PVP-2.5, C) PAA-PVP-5, D) PAA-PVP-7.5, E) PAA-PVP-10.

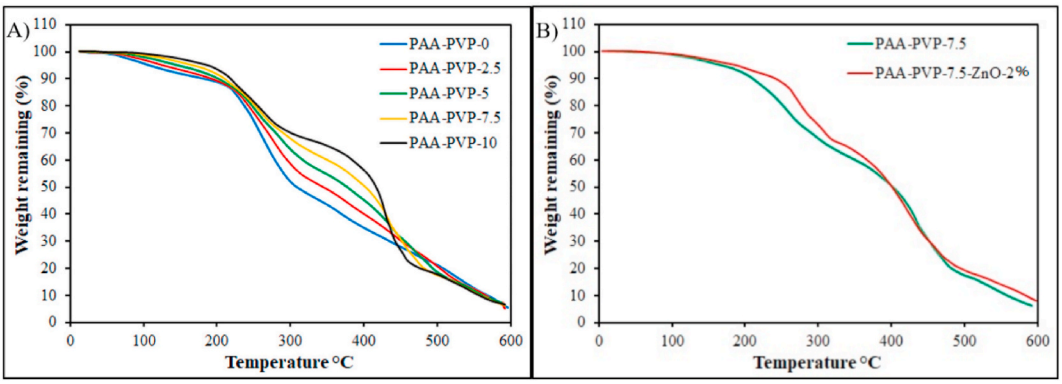

Fig. 5. (A) TGA thermograms of PAA-based hydrogels containing various amounts of PVP changes in thermal degradation profile as weight percent. (B) Comparison of TGA analysis between PAA-PVP-7.5 and PAA-PVP-7.5-ZnO-2%.

Fig. 6. XRD analysis was used to investigate how the nanoparticles are dispersed (whether they are clumped or well dispersed) in the hydrogel. As shown in Fig. 6, the peaks of the zinc oxide index are evident in areas 34, 37, 39, 50, 59, and 70 2θ [41,42]. None of these peaks are seen in the PAA-PVP-7.5 sample, whereas adding ZnO to the hydrogel makes these peaks more intense, making the acrylic acid chains more regular. In addition, PAA-PVP-7.5-ZnO-2% hydrogel has conformity with the ZnO nanoparticles diagram as a reference, emphasizing the presence and reasonable distribution of ZnO in the hydrogel structure.

The Debye-Scherer equation, which shows a relationship between the broadening of the peak in XRD and the particle size, can be used to estimate the average particle size of zinc oxide nanoparticles. As shown below:

$$D = k\lambda/\beta\cos\theta$$

Where D is the crystal particle size, k is Scherer's constant (0.9), λ is the X-ray wavelength (copper source, 0.15406 nm), β is the XRD peak width at half height, and θ is the Bragg diffraction angle. The average crystal size of ZnO nanoparticles was calculated and found to be (46.30–36.29 nm). It was proved that pure ZnO nanoparticles were loaded in PAA-PVP-7.5-ZnO Hydrogel.

3.7. SEM & EDAX results of PAA-PVP-7.5-ZnO-2% hydrogel

The SEM images of the hydrogel containing nanoparticles show the distribution of nanoparticles in the hydrogel, and the XRD diagram confirmed the results. Fig. 7 (A&B) shows the images of ZnO nanoparticles in two different magnifications, whose size distribution is shown in Fig. 7G, which is below 200 nm. The difference between SEM and XRD results is related to SEM images, nanoparticles may combine together, and some particles appear coarse because they were imaged in a dry state. Comparison of nanoparticles in hydrogel Fig. 7(E&F) with the control groups, which did not contain ZnO Fig. 7(C&D), illustrate ZnO particles as clumps on the refraction surface of the image. Also, the EDAX results are represented in Fig. 7 (H&I), which show the presence of the ZnO element in Fig. 7I, whereas this peak is not observed in Fig. 7H.

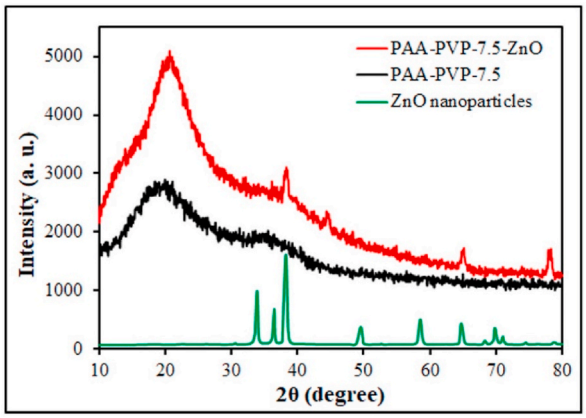

Fig. 6. XRD patterns of PAA-PVP-7.5, PAA-PVP-7.5-ZnO-2% hydrogels, and ZnO nanoparticles.

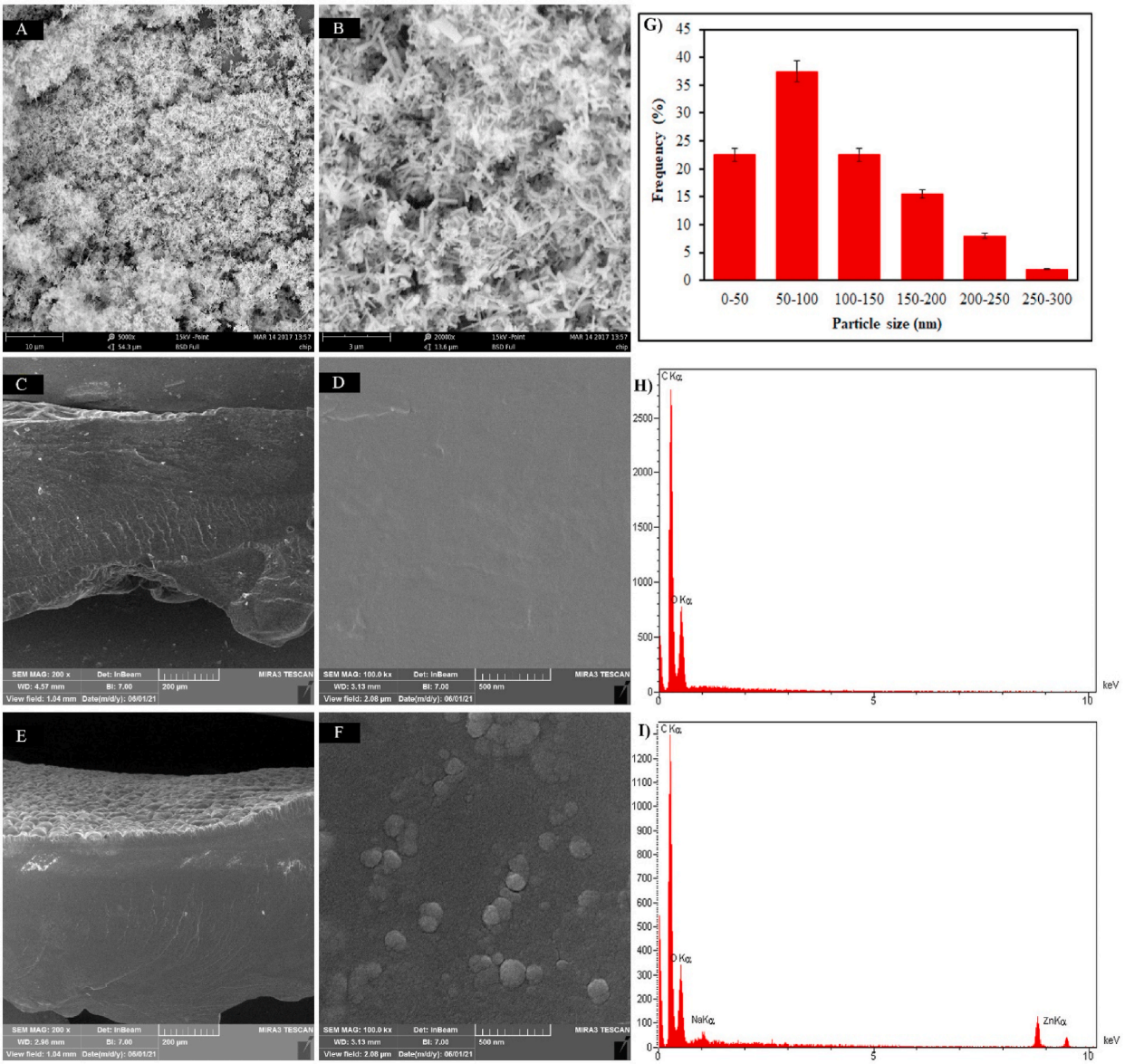

Fig. 7. SEM micrographs, particle size distribution curves, and EDX analysis. (A&B) SEM of ZnO nanoparticles. (G) particle size distribution curves of ZnO nanoparticles, (C&D) control groups without ZnO nanoparticles, (E) and (F) hydrogels with ZnO nanoparticles, (H) Edax diagram Hydrogel without ZnO nanoparticles, and (I) Edax diagram Hydrogel with ZnO nanoparticles.

3.8. Antibacterial test results

According to Fig. 8C, PAA-PVP-7.5-ZnO-2% did not show a significant difference with Getamycin in both S. aureus and P. aeruginosa strains.

3.9. Cytocompatibility of PAA-PVP-7.5-ZnO-2% hydrogel

The cytocompatibility of the hydrogel was determined using the MTT assay. No cytotoxic effects were observed, as shown in Fig. 9. Surprisingly, the PAA-PVP-7.5-ZnO-2% hydrogel increased the proliferation rate of HDF. Overall, these findings indicate that the PAA-PVP-7.5-ZnO-2% hydrogel has healing properties.

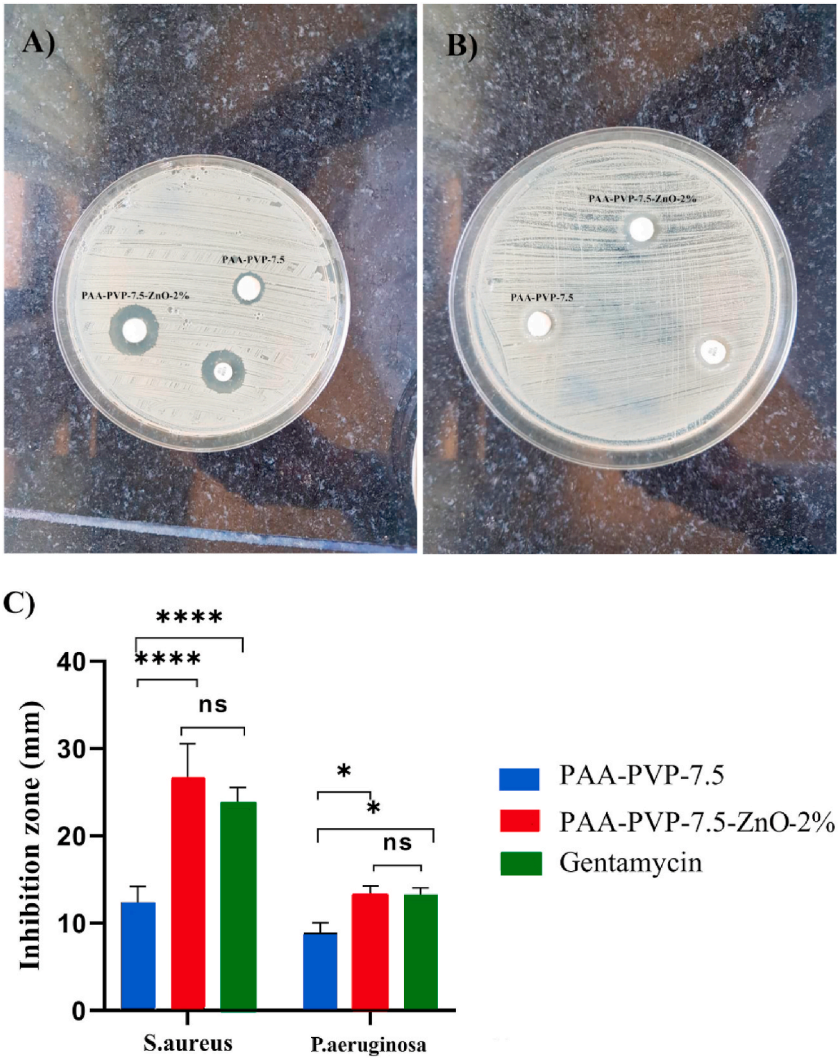

Fig. 8. Antibacterial activity of hydrogels: (A) inhibition zone of *S. aureus* generated by PAA-PVP-7.5 and PAA-PVP-7.5-ZnO-2%. (B) inhibition zone of P. seudomonas generated by PAA-PVP-7.5 and PAA-PVP-7.5-ZnO-2%.(C) Bar graph responding to the size of the zone of inhibition formed around each disc.

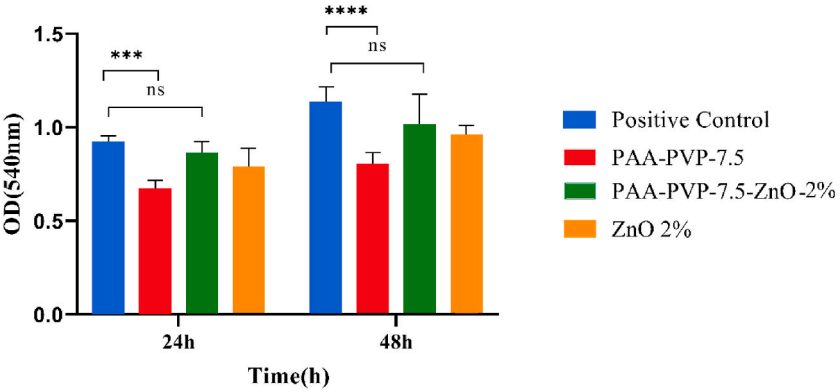

Fig. 9. In vitro cytotoxicity test of the hydrogels on human dermal fibroblast cell line (HDF) after 24 and 48 h.

3.10. PAA-PVP-7.5 hydrogel containing ZnO effectively improves wound healing

The extent of wound closure was photographed on days 0, 7, and 21 post-surgery. As shown in Fig. 10A, from days 7 to 21, wound contraction was greater in the PAA-PVP-7.5-ZnO-2% group than in the control group. On day 21, complete wound closure was observed in the PAA-PVP-7.5-ZnO-2% group, whereas the lowest repair occurred in the control group. The percentage of wound contraction was quantified 7 and 21 days after surgery. As shown in Fig. 10B, the PAA-PVP-7.5-ZnO-2% group had the highest percentage of wound contraction, which was significantly ($p < 0.0001$) higher than the control group at all time points.

As shown in Fig. 10C, histological analysis of the healing area demonstrated partial epithelialization from the wound edge toward the center on day 7 in control and treatment groups. Complete multi-layer epithelialization was observed on day 21 in PAA-PVP-7.5-ZnO-2%. Of note, unlike the PAA-PVP-7.5-ZnO-2% group, the formation of dried exudate and lack of air circulation and moisture

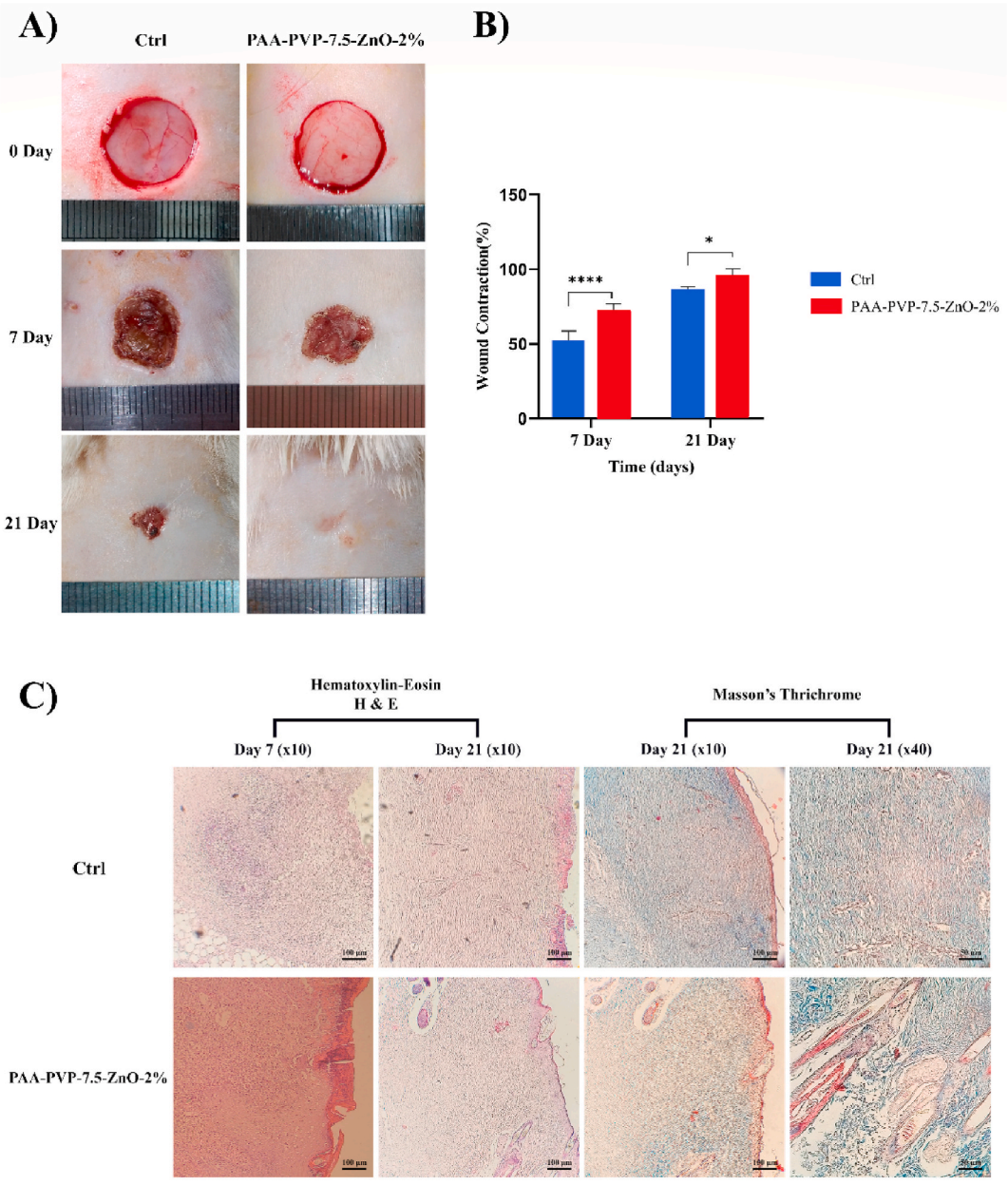

Fig. 10. Macroscopic presentation, statistical analysis and microscopic presentation of excisional wound at various time intervals. (A) Pictures show defected area in different groups at 7 and 21 days. (B) Wound contraction percent was measured by ANOVA test ***$P < 0.001$, **$P < 0.01$. The number of replications = at least 10. (C) Photomicrographs presentation of wound area histologically by H & E and Masson's trichrome staining scale bar = 100 μm.

retention in the Ctrl group prevented complete epithelialization. In other words, these results strongly suggest that PAA-PVP-7.5-ZnO-2% hydrogel had an active role in absorbing blood and exudate. The presence of dense nuclei in the control group is a sign of tissue inflammation compared to PAA-PVP-7.5-ZnO-2% group on day 7. It is worth noting that, the morphology of the epithelium in PAA-PVP-7.5-ZnO-2% group is structurally similar to the normal skin epithelium. Supporting this notion, the PAA-PVP-7.5-ZnO-2% group has been involved in the enhancement of keratinocyte proliferation and migration. Also, on day 21, the presence of sebaceous glands and hair follicles in the PAA-PVP-7.5-ZnO-2% group is evident. In order to evaluate collagen arrangement, Masson's trichrome staining was used Fig. 10. Interestingly, the thickness and arrangement of collagen in the PAA-PVP-7.5-ZnO-2% group was better than the Ctrl group, suggesting a high efficacy of in PAA-PVP-7.5-ZnO-2% in wound healing.

4. Conclusion

In order to improve the quality of wound healing, we designed a new hydrogel wound dressing containing ZnO nanoparticles and examined its potential healing capacity in the animal trial. Our findings in the analysis of PAA-PVP-7.5-ZnO-2% hydrogel showed that the uniform distribution of ZnO inside the hydrogel exerts effective antibacterial activities. Also, the advantages of this novel hydrogel, such as biocompatibility, absorption of exudate due to optimal porosity, and controlled release improve rat excisional injury. In this regard, however, additional and comprehensive studies are required. Furthermore, studies on the safety and efficacy of this wound dressing in other skin injuries, such as burns, diabetic ulcers, bedsores, abnormalities such as epidermolysis bullosa, and traumatic injuries, can reveal different potentials of this wound dressing, and its clinical trial phases can be effective in terms of appropriate clinical use of this wound dressing.

Author contributions

Zahra Pourmohammadi-Bejarpasi: Conceived and designed the experiments, performed the experiments, analyzed and interpreted the data, contributed reagents, materials, analysis tools or data, and wrote the paper.

Alireza Feizkhah: Performed the experiments, and contributed reagents, materials, analysis tools or data.

Mohammadreza Mobayen: Performed the experiments, and contributed reagents, materials, analysis tools or data.

Mojtaba Hedayati: Performed the experiments, and contributed reagents, materials, analysis tools or data.

Mahsa Sadeghi: Performed the experiments, contributed reagents, materials, analysis tools or data, and wrote the paper.

Mojdeh Esmaelzadeh: Methodologist, analysis tools or data, and wrote the paper.

Fatemeh Beygom Mirkatoul: Performed the experiments, contributed reagents, materials, analysis tools or data.

Solma Jamshidi: Performed the experiments, and contributed reagents, materials, analysis tools or data.

Mohsen Shahrousvand: Conceived and designed the experiments, performed the experiments, analyzed and interpreted the data, contributed reagents, materials, analysis tools or data, and wrote the paper.

Seyyedeh Sahra Mirmasoudi: Conceived and designed the experiments, performed the experiments, analyzed and interpreted the data, contributed reagents, materials, analysis tools or data, and wrote the paper.

Declaration of competing interest

The authors declare that they have no known competing financial interests or personal relationships that could have appeared to influence the work reported in this paper.

Acknowledgements

This study was supported by Guilan University of Medical Sciences (Grant number: IR. GUMS.REC.1400.425). The authors are also thankful to Mr. Emad Jafari-Bejarbane for their help during the in vivo study.

References

[1] L. Amani, S. Soleymanzadeh Moghadam, M. Roudbari, R. Roustapoor, M. Armat, A. Rastegar Lari, Epidemiology and mortality of burned patients referred to motahari hospital, tehran, Razi J. Med. Sci. 21 (2015) 31–38.
[2] G. Zikaj, G. Belba, G. Xhepa, Epidemiology of hand burn in Albania 2011-2016, Open Acc. Maced. J. Med. Sci. 6 (2018) 931.
[3] A. Clark, J. Imran, T. Madni, S.E. Wolf, Nutrition and metabolism in burn patients, Burn. trauma 5 (2017).
[4] L. Horkan, G. Stansfield, M. Miller, An analysis of systematic reviews undertaken on standard advanced wound dressings in the last 10 years, J. Wound Care 18 (2009) 298–304, https://doi.org/10.12968/jowc.2009.18.7.43113.
[5] I.R. Sweeney, M. Miraftab, G. Collyer, A critical review of modern and emerging absorbent dressings used to treat exuding wounds, Int. Wound J. 9 (2012) 601–612, https://doi.org/10.1111/j.1742-481X.2011.00923.x.
[6] R.J. Morin, N.L. Tomaselli, Interactive dressings and topical agents, Clin. Plast. Surg. 34 (2007) 643–658, https://doi.org/10.1016/j.cps.2007.07.004.
[7] N. Kashyap, N. Kumar, M.N.V.R. Kumar, Hydrogels for pharmaceutical and biomedical applications, Crit. Rev. Ther. Drug Carrier Syst. 22 (2005).
[8] S. Mignani, S. El Kazzouli, M. Bousmina, J.-P. Majoral, Expand classical drug administration ways by emerging routes using dendrimer drug delivery systems: a concise overview, Adv. Drug Deliv. Rev. 65 (2013) 1316–1330.
[9] Y. Tanaka, J.P. Gong, Y. Osada, Novel hydrogels with excellent mechanical performance, Prog. Polym. Sci. 30 (2005) 1–9.
[10] W.W.J. Unger, A.J. Van Beelen, S.C. Bruijns, M. Joshi, C.M. Fehres, L. Van Bloois, M.I. Verstege, M. Ambrosini, H. Kalay, K. Nazmi, Glycan-modified liposomes boost CD4+ and CD8+ T-cell responses by targeting DC-SIGN on dendritic cells, J. Contr. Release 160 (2012) 88–95.
[11] Y. Luo, J.B. Kobler, J.T. Heaton, X. Jia, S.M. Zeitels, R. Langer, Injectable hyaluronic acid-dextran hydrogels and effects of implantation in ferret vocal fold, J. Biomed. Mater. Res. Part B Appl. Biomater. 93 (2010) 386–393.

[12] Q.V. Nguyen, J.H. Park, D.S. Lee, Injectable polymeric hydrogels for the delivery of therapeutic agents: a review, Eur. Polym. J. 72 (2015) 602–619.
[13] J. Radhakrishnan, U.M. Krishnan, S. Sethuraman, Hydrogel based injectable scaffolds for cardiac tissue regeneration, Biotechnol. Adv. 32 (2014) 449–461.
[14] T. Thambi, Y. Li, D.S. Lee, Injectable hydrogels for sustained release of therapeutic agents, J. Contr. Release 267 (2017) 57–66.
[15] A.S. Hoffman, Adv. Drug Deliv. Rev. 54 (2002) 3–12.
[16] G. Bisht, S. Rayamajhi, ZnO nanoparticles: a promising anticancer agent, Nanobiomedicine 3 (2016) 3–9.
[17] J.C. Dumville, S. O'Meara, S. Deshpande, K. Speak, Hydrogel dressings for healing diabetic foot ulcers, Cochrane Database Syst. Rev. (2013).
[18] J.G. Powers, L.M. Morton, T.J. Phillips, Dressings for chronic wounds, Dermatol. Ther. 26 (2013) 197–206.
[19] X. Xu, Y. Zeng, Z. Chen, Y. Yu, H. Wang, X. Lu, J. Zhao, S. Wang, Chitosan-based multifunctional hydrogel for sequential wound inflammation elimination, infection inhibition, and wound healing, Int. J. Biol. Macromol. 235 (2023), 123847.
[20] J. Zhang, J. Hu, B. Chen, T. Zhao, Z. Gu, Superabsorbent poly (acrylic acid) and antioxidant poly (ester amide) hybrid hydrogel for enhanced wound healing, Regen. Biomater. 8 (2021) rbaa059.
[21] X.Y. Chen, H.R. Low, X.Y. Loi, L. Merel, M.A. Mohd Cairul Iqbal, Fabrication and evaluation of bacterial nanocellulose/poly (acrylic acid)/graphene oxide composite hydrogel: characterizations and biocompatibility studies for wound dressing, J. Biomed. Mater. Res. Part B Appl. Biomater. 107 (2019) 2140–2151.
[22] J. Koehler, L. Wallmeyer, S. Hedtrich, A.M. Goepferich, F.P. Brandl, PH-modulating poly (ethylene glycol)/alginate hydrogel dressings for the treatment of chronic wounds, Macromol. Biosci. 17 (2017), 1600369.
[23] T.S. Stashak, E. Farstvedt, A. Othic, Update on wound dressings: indications and best use, Clin. Tech. Equine Pract. 3 (2004) 148–163.
[24] C. Trial, H. Darbas, A. Sotto, G. Simoneau, Y. Tillet, Assessment of the Antimicrobial Effectiveness of a New Silver Alginate Wound Dressing: A RCT. 20–26, 2002.
[25] K. Ali, S. Dwivedi, A. Azam, Q. Saquib, M.S. Al-Said, A.A. Alkhedhairy, J. Musarrat, Aloe vera extract functionalized zinc oxide nanoparticles as nanoantibiotics against multi-drug resistant clinical bacterial isolates, J. Colloid Interface Sci. 472 (2016) 145–156, https://doi.org/10.1016/j.jcis.2016.03.021.
[26] M. Kaushik, R. Niranjan, R. Thangam, B. Madhan, V. Pandiyarasan, C. Ramachandran, D.-H. Oh, G.D. Venkatasubbu, Investigations on the antimicrobial activity and wound healing potential of ZnO nanoparticles, Appl. Surf. Sci. 479 (2019) 1169–1177.
[27] K. Huang, Z. Jinzhong, T. Zhu, Y. Morsi, A. Aldalbahi, M. El-Newehy, X. Yan, X. Mo, Exploration of the antibacterial and wound healing potential of a PLGA/silk fibroin based electrospun membrane loaded with zinc oxide nanoparticles, J. Mater. Chem. B 9 (2021) 1452–1465.
[28] S.M.I. Rayyif, H.B. Mohammed, C. Curuțiu, A.C. Bîrcă, A.M. Grumezescu, B. Ștefan Vasile, L.M. Dițu, V. Lazăr, M.C. Chifiriuc, G. Mihăescu, ZnO nanoparticles-modified dressings to inhibit wound pathogens, Materials 14 (2021) 3084.
[29] Y. Xiang, X. Qi, E. Cai, C. Zhang, J. Wang, Y. Lan, H. Deng, J. Shen, R. Hu, Highly efficient bacteria-infected diabetic wound healing employing a melanin-reinforced biopolymer hydrogel, Chem. Eng. J. 460 (2023), 141852.
[30] S. Cheng, H. Wang, X. Pan, C. Zhang, K. Zhang, Z. Chen, W. Dong, A. Xie, X. Qi, Dendritic hydrogels with robust inherent antibacterial properties for promoting bacteria-infected wound healing, ACS Appl. Mater. Interfaces 14 (2022) 11144–11155.
[31] X. Qi, Y. Xiang, E. Cai, S. You, T. Gao, Y. Lan, H. Deng, Z. Li, R. Hu, J. Shen, All-in-One: harnessing multifunctional injectable natural hydrogels for ordered therapy of bacteria-infected diabetic wounds, Chem. Eng. J. 439 (2022), 135691.
[32] D. Simões, S.P. Miguel, M.P. Ribeiro, P. Coutinho, IJ Correia Mendonça, Eur. J. Pharm. Biopharm. 127 (2018) 130.
[33] R. Nagasaka, C. Chotimarkorn, I.M. Shafiqul, M. Hori, H. Ozaki, H. Ushio, Anti-inflammatory effects of hydroxycinnamic acid derivatives, Biochem. Biophys. Res. Commun. 358 (2007) 615–619.
[34] Z. Pourmohammadi-Bejarpasi, R. Sabzevari, A.M. Roushandeh, A. Ebrahimi, M. Mobayen, A. Jahanian-Najafabadi, A. Darjani, M.H. Roudkenar, Combination therapy of metadichol nanogel and lipocalin-2 engineered mesenchymal stem cells improve wound healing in rat model of excision injury, Adv. Pharmaceut. Bull. 12 (2022) 550.
[35] B. Mirani, E. Pagan, B. Currie, M.A. Siddiqui, R. Hosseinzadeh, P. Mostafalu, Y.S. Zhang, A. Ghahary, M. Akbari, An advanced multifunctional hydrogel based dressing for wound monitoring and drug delivery, Adv. Healthcare Mater. 6 (2017), 1700718.
[36] M.A.Q. Bhuiyan, M. Rahman, M.S. Rahaman, M. Shajahan, N.C. Dafader, Improvement of swelling behaviour of poly (vinyl pyrrolidone) and acrylic acid blend hydrogel prepared by the application of gamma radiation, Org. Chem. Curr. Res. 4 (2015) 401–2161.
[37] Y. Wu, L.-D. Liao, H.-C. Pan, L. He, C.-T. Lin, M.C. Tan, Fabrication and interfacial characteristics of surface modified Ag nanoparticle based conductive composites, RSC Adv. 7 (2017) 29702–29712.
[38] M. Demeter, V. Meltzer, I. Călina, A. Scărișoreanu, M. Micutz, M.G.A. Kaya, Highly elastic superabsorbent collagen/PVP/PAA/PEO hydrogels crosslinked via e-beam radiation, Radiat. Phys. Chem. 174 (2020), 108898.
[39] A. Majeed, F. Pervaiz, H. Shoukat, K. Shabbir, S. Noreen, M. Anwar, Fabrication and evaluation of PH sensitive chemically cross-linked interpenetrating network [Gelatin/Polyvinylpyrrolidone-Co-poly (acrylic acid)] for targeted release of 5-fluorouracil, Polym. Bull. 1–20 (2020).
[40] R.C. Mundargi, V. Rangaswamy, T.M. Aminabhavi, Poly (N-vinylcaprolactam-Co-methacrylic acid) hydrogel microparticles for oral insulin delivery, J. Microencapsul. 28 (2011) 384–394.
[41] S. Yedurkar, C. Maurya, P. Mahanwar, Biosynthesis of zinc oxide nanoparticles using ixora coccinea leaf extract—a green approach, Open J. Synth. Theor. Appl. 5 (2016) 1–14.
[42] S. Talam, S.R. Karumuri, N. Synthesis Gunnam, Characterization, and spectroscopic properties of ZnO nanoparticles, Int. Sch. Res. Notices 2012 (2012).